4-15-1991

# Transport Properties of an Interacting Lattice Gas Model in a Charge Density Gradient by Monte Carlo Simulation

Ras B. Pandey
*University of Southern Mississippi*, ras.pandey@usm.edu

Songping Gao
*University of Southern Mississippi*

# Transport properties of an interacting-lattice-gas model in a charge-density gradient by Monte Carlo simulation

Ras Pandey and Songping Gao*
*Department of Physics and Astronomy, University of Southern Mississippi, Hattiesburg, Mississippi 39406*
(Received 16 August 1990; revised manuscript received 21 December 1990)

A two-dimensional lattice is considered with a linear charge-density gradient produced by a charge source at one end and a sink at the opposite end. A fraction $p$ of the lattice sites are occupied by mobile particles that interact only with neighboring particles and empty sites (the substrate) and carry charges from source to sink; the charge neutrality of the whole lattice is maintained. The root-mean-square (rms) displacement of the particles (i.e., the tracers) and their effective conductivity for the charge transport are studied as a function of temperature and concentration $p$. The rms displacement shows a crossover from diffusion (at short time) to driftlike behavior (in the long-time regime). The effective conductivity depends nonmonotonically on the carriers' concentration, in which two maxima peaks are observed; the peak at the higher concentration seems to characterize the onset of static percolation. At a fixed concentration, the conductivity remains almost constant at low temperatures and increases before it saturates to a higher value in the high-temperature regime. In the intermediate-temperature range, an Arrhenius dependence seems valid at high concentrations; however, a deviation on varying the concentration cannot be ruled out at low concentration. We find that the activation energy depends on carrier concentration and temperature.

## I. INTRODUCTION

Understanding the transport properties of interacting particles (i.e., the lattice gas), ions, and inonomers has been an area of continuous interest experimentally[1-6] as well as theoretically.[7-10] Because of enormous applicability, such as processing of various additives into polymers, ion separation and filtering through membranes in a variety of aqueous solutions, producing a sol-gel system of a ramified network with a desired distribution of branches and loops, etc., the experimental investigation of the diffusion of the penetrant molecules has attracted considerable interest in recent years.[3,4] Particularly, the diffusion of various dialkyl phthalate plasticizers such as di-*n*-octyl phthalate (DNOP), di-*n*-hexyl phthalate (DNHxP), diundecyl phthalate (DUP), etc., in polyvinyl chloride (PVC) has been recently studied by Storey, Mauritz, and Cox[4] by a mass uptake technique. They find[4] that the diffusion coefficient shows an Arrhenius dependence on temperature; however, the activation energy below the glass transition temperature was found to be different from the activation energy above it, depending on the nature of the host substrate. The motion of the penetrant molecules (i.e., the plasticizers) may be affected by many factors, such as the molecular weight, ion content, ion distribution, counter ions, etc., and it is rather difficult to isolate the effects of each factor in such a highly interacting system. Therefore, it is important to investigate simple models for the interacting systems to gain a physical insight into some of the most difficult issues on the transport phenomenon.

Despite a number of theoretical attempts,[8,9] our understanding of the basic problems of transport in such a complex interacting system is limited. Because of the intractabilities of the analytical tools,[8,9] most of the theoretical attempts have been restricted to simplified models, such as single-particle diffusion, lattice gas with hard-core interaction, dilute lattice gas, etc. Computer-simulation methods,[10-19] on the other hand, have added a lot to our understanding of a variety of transport processes—for example, anomalous diffusion in random percolating systems, scaling of conductivity in stirred percolations, tracer diffusion in lattice-gas models of two-component systems, interdiffusion and motion governed by their correlated hopping rates, and diffusive front in a gradient-induced percolation. Such computer experiments are also constrained to simple systems due to machine limitations on memory and execution time. One of the most complex problems that has attracted a great deal of attention is transport in Coulomb gas,[18-20] and what makes it difficult to deal with is the long-range interaction that leads to long relaxation time.[18] In order to gain insight into the transport quantities like rms displacement and effective conductivity in such an interacting system, we have recently studied an interacting-lattice model[19] in which the effect of the range of interaction and screening is addressed. Although we have considered transport of particles which interact with each other and with the host that acts as an oppositely charged background in a charge-density gradient, the effect of temperature was not considered at all. Here we investigate the effect of temperature and concentration on the transport quantities but restrict ourselves to the nearest-neighbor interactions. In Sec. II we describe the model and we present the results in Sec. III. A summary and discussion are provided in Sec. IV.

 

## II. MODEL

As in our previous study,[19] we consider a two-dimensional discrete lattice of size $L_x \times L_y$ (see Fig. 1). One end of the lattice (say, the first column) is connected with a charge source, while the opposite end along the $x$ axis (the $L_x$th column) is connected by a sink. A fraction $p$ of the lattice sites is randomly occupied by particles, the charge carriers, leaving a fraction $(1-p)$ of lattice sites empty. A lattice site cannot be occupied by more than one particle and this introduces a hard-core interaction among the particles. Each particle, in contact with the source, i.e., a particle on any site of the first column, is assigned a unit charge density, while those in contact with sink (i.e., on the $L_x$th column) are assigned a zero charge density; the rest of the particles are assigned charge densities (0 or 1) to achieve a linear charge-density gradient of 1 at the source and 0 at the sink, i.e., $\nabla\rho_x \sim 1/L_x$. Each empty site (i.e., the hole) is assigned a charge density of an opposite sign to maintain the charge neutrality of the whole system. Thus, if there are $N_c$ charged particles in the system, then the charge density of each empty site is

$$\rho_v = -N_c/N_v \ , \tag{1}$$

where $N_v = (1-p)L_xL_y$ is the number of vacant sites. The charges spread over vacant sites thus act as background charges of the substrate. The sample is now initialized and ready for studying the transport properties.

Each particle interacts with its neighboring particles with a repulsive interaction and with its neighboring empty sites (the substrate) with an attractive interaction. The hopping of a particle depends on the interaction energy, the technical details of which are described in the following. A particle at site $i$ and one of its neighbors, say, site $j$, are selected randomly (see Fig. 2). If site $j$ is

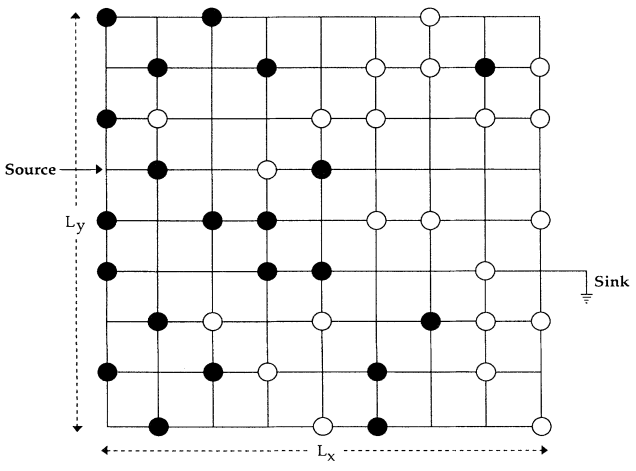


FIG. 1. Schematic representation of the two-dimensional lattice model. Particles are shown by circles in which solid circles represent charged particles and open circles, the neutral particles. The empty sites (without circles) are oppositely charged to maintain the charge neutrality.

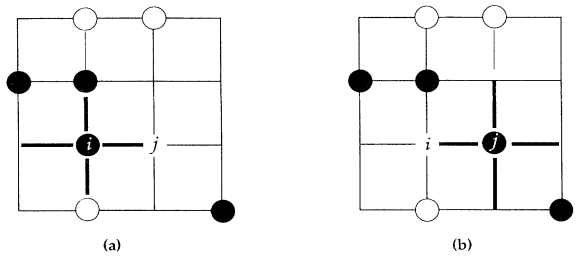


FIG. 2. Hopping of a particle from site $i$, in its current configuration (a) to a neighboring site $j$ in its new configuration (b). The energy of the particle $E_0$ in configuration (a) and $E_1$ in configuration (b) is calculated from its interaction with its neighbors shown by heavy lines using Eq. (2).

empty, then we calculate (i) the interaction energy $E_0$ with the particle at site $i$,

$$E_0 = \rho_i \sum_k \rho_k \ , \tag{2}$$

where the summation index $k$ runs over all the neighboring particles and holes [connected by nearest-neighbor bonds from site $i$; see Fig. 2(a)] and $\rho_k$ is the charge density of the particle or hole at the neighboring site $k$. Note that, for a particle at site $k$, $\rho_k$ may be either 1 or 0, while for a hole, it may be a noninteger number, depending upon the concentration $(1-p)$ of the holes and the number of charge particles. (ii) The interaction energy $E_1$ is evaluated for a configuration (Fig. 2) in which particle and hole positions as well as their charges are exchanged [Fig. 2(b)], and then (iii) we evaluate the change in energy $\Delta E = E_1 - E_0$. If the change $\Delta E \leq 0$, then the new configuration is accepted, and the particle is moved from site $i$ to site $j$. If $\Delta E = 0$, then the new configuration for the particle's hop is accepted with a Boltzmann distribution, $\exp(-\Delta E/k_BT)$, as in the Metropolis algorithm.[21] On the other hand, if site $j$ is occupied, then the particle stays at site $i$ and steps (i) through (iii) are not executed.

When these energetic conditions are favorable, the particle moves from site $i$ to site $j$, which is accompanied by a charge transfer depending upon the charge density of the particle and location of these sites. If site $j$ is at the first column (connected by the source), then the charge transfer $(1-\rho_j)$ is counted as the amount of charge released from the source and the charge density $\rho_j$ of this particle at site $j$ is set to unity. Similarly, if the $j$th site belongs to the $L_x$th column (connected by the sink), then the charge transfer $\rho_j$ is added to the total charge absorbed by the sink and the charge density $\rho_j$ is set to 0. Thus the charges can be transferred from source to sink, as the carriers execute their stochastic motion. This process of selecting a particle and its neighboring site randomly, attempting to move it and updating its charge density, is repeated again and again for all the particles. Each attempt, irrespective of its success in moving a particle, is counted in the Monte Carlo (MC) time step,[21] and an attempt to move each particle once on average is defined as one MC step (MCS). The simulation is performed for a preset (large) number of MCS, which is the

total length of time scale in our computer experiment. The periodic boundary condition is imposed for the motion along the $y$ direction, while the open boundary condition is used along the $x$ direction at the source and the sink.

During the simulation, we keep track of the following quantities: (1) charges released from the source $Q_1(t)$, (2) charges absorbed at the sink $Q_2(t)$, (3) rms displacement of the particles (i.e., tracers) and (4) the rms displacement of the center of mass of the particle system at each time step. A limited number of these quantities are, however, printed periodically at equal intervals of time. Although we produce most of our data with the sample size $60\times60$, we have used different sizes to test the reliability of our data. The time scales range from $10^5$ to $3\times10^5$ MCS, although most of the data we run at the maximum time steps. In steady-state equilibrium, the amount of charge released from the source must be nearly the same as that absorbed at the sink. The relaxation time, to approach its steady state in which the charge released from the source equals the charge absorbed at the sink, depends on the concentration of the carriers; the higher the concentration, the longer the relaxation time. We also observe that the relaxation time increases sharply on lowering the temperature. Most of the data presented here are in the regime where the system had reached the steady state.

## III. RESULTS AND DISCUSSION

All the transport quantities mentioned in Sec. II are studied as a function of the carrier concentration $p$ and temperature $\tau=k_BT$. Although our primary interest is in the variation of the effective conductivity with $p$ and $\tau$, we do keep track of some other auxiliary quantities, as we see in the following.

### A. rms displacements

To gain insight into the overall geometry of the medium (self-similar inhomogeneous random and homogeneous media, in particular) and the effect of interactions with the medium, and of the local and global external fields, it is often useful to analyze the dependence of the rms displacement of the particles on time. In fact, the asymptotic exponent for the variation of the rms displacement with time and its prefactor have been widely used[12–14] for evaluating the conductivity exponents and diffusion constant which depend on the medium. In our model study here, we have looked into the rms displacement $R_{\rm tr}$ of the carriers, i.e., the tracers, individually as well as collectively, and the rms displacement $R_{\rm c.m.}$ of the center of mass of the carriers. A typical variation of $R_{\rm c.m.}$ with time $t$ is shown in Fig. 3(a). As the carriers execute their stochastic motion, their center of mass hops around randomly in the charge-density gradient from source to sink. The rms displacement $R_{\rm c.m.}$ at a time step $t$ describes the instantaneous distribution of the particles and it is a measure of polarization. Variation in the center of mass $R_{\rm c.m.}$ of carriers shows the variation in polarization in field induced by the charge-density gradient.

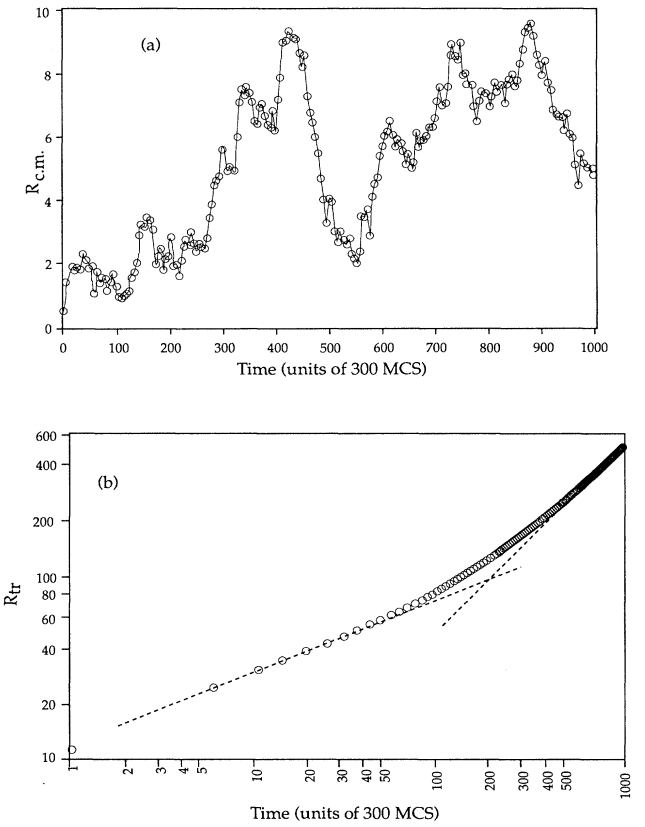


FIG. 3. (a) rms displacement vs time of the center of mass (of the carriers) and (b) of the tracers on a log-log plot, at concentration $p=0.4$, and $\tau=0.8$ on a sample $60\times60$.

We see that $R_{\rm c.m.}$ increases systematically with some fluctuations, during the initial time region (up to about $1.3\times10^5$ MCS). This provides an average estimate of the response time in which most of the carriers have traveled across the sample (i.e. from source to sink) and have reflected back, leading to an abrupt fall in the magnitude of the $R_{\rm c.m.}$. Similar patterns of growth and decay appear over almost the same period of time.

The rms displacement of the tracer, $R_{\rm tr}$, on the other hand, increases continuously with time [Fig. 3(b)]. It is, however, apparent from Fig. 3(b) that the rms displacement has a different slope in short- and long-time regimes. This implies that there are two power-law dependences for $R_{\rm tr}$, i.e.,

$$R_{\rm tr}=D_1t^{k_1}+D_2t^{k_2}\ , \tag{3}$$

where exponents $k_1$ and $k_2$ describe the motion of tracers in short- and long-time regimes, respectively, with corresponding prefactors $D_1$ and $D_2$. Both exponents seem to depend on temperature and carrier concentration. At very low concentration and high temperature, the magnitude of the exponent $k_1$ is close to $\frac{1}{2}$, showing a diffusionlike motion. However, at low temperature and high concentration, $k_1$ is appreciably smaller than $\frac{1}{2}$, the diffusive value. For example, at $p=0.1$ and $\tau=0.4$,

$k_1=0.47\pm0.02$; at $p=0.35$ and $\tau=0.01$, $k_1=0.41\pm0.02$. The exponent $k_2$ seems to approach its drift value of 1 in the long-time regime; the time to approach this regime, i.e., the relaxation time, increases on increasing the concentration and lowering the temperature.

We would like to point out that the short-time regime is determined by the rms displacement bounded by the length of the sample. In other words, the upper cutoff for the short-time regime is the time in which a tracer, on average, has gone from one end of the sample to the other. In the long-time regime, on the other hand, tracers have made numerous trips from source to sink (along the direction of gradient field) leading to a faster motion; in this long-time regime, the length of the sample may be considered as the unit step of the motion. It is rather difficult to understand the nondiffusive nature of transport in the short-time regime due to the appearance of correlation length which depends on carrier concentration and temperature. A detailed quantitative analysis of the power-law behavior of the rms displacements is under investigation and will be published later as results become available.

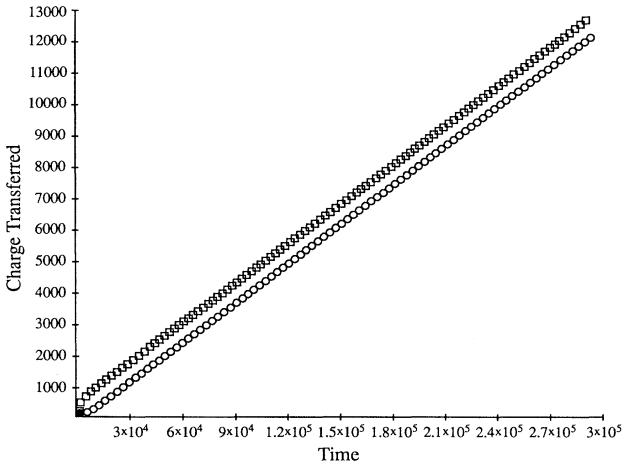


FIG. 4. Charge transfer at the source (□) and at the sink (○) vs time, for the same parameters as in Fig. 1.

### B. Charge transferred and the effective conductivity

In addition to particle transport, we consider a charge transfer from source to sink in our model, as described in Sec. II. The interacting particles are in constant stochastic motion, and they carry charges from source to sink. In steady state, the equilibrium distribution of the charged particles leads to a linear charge-density gradient (1 at the source and 0 at the sink). The time required to reach the steady state depends on the initial distribution of the charged particles, the total concentration $p$ of the particles, and the temperature $\tau$. The relaxation time increases on increasing the concentration $p$ and decreases on raising the temperature. To reduce the relaxation time, we initialize the sample by distributing the charged particles in such a way that an approximate linear charge density is established before the hopping of the particles begins.

The total amount of charge transfer from source to sink depends on temperature and on carrier concentration. In the steady state, the amount of charge released from the source should be equal to the amount of charge absorbed at the sink at any time step. A typical plot of the charge $Q_r$ released from the source and the number of charge $Q_a$ absorbed at the sink versus time is shown in Fig. 4. We see that $Q_r$ is not the same as $Q_a$ in steady state; however, the difference $\Delta Q=(Q_r-Q_a)$ remains nearly the same throughout the steady-state regime. This discrepancy, the amount $\Delta Q$, is the charge which remains uncounted in the bulk because we count only the charges released from the source and that absorbed at the sink. The amount of uncounted charge in the bulk $\Delta Q$ depends on temperature and the carrier concentration $p$.

Let us now define the effective conductivity in our model. The charge transport across the sample along the $x$ direction leads to a current,

$$I=\frac{dQ}{dt} . \tag{4}$$

In the steady state, the current density

$$j=I/L_x=\sigma E , \tag{5}$$

where $\sigma$ is the effective conductivity and $E$ is an effective field produced by the charge-density gradient. If $E\sim\nabla\rho(x)\sim 1/L_x$ in steady state, then from Eqs. (4) and (5) we find

$$\sigma=(L_x/L_y)\frac{dQ}{dt} . \tag{6}$$

Thus, by calculating the slope of the $Q(t)$ versus $t$ plot, we can estimate the effective conductivity. We should point out here that the word "effective conductivity" is used to explore the charge transport; it may not be equal to the absolute conductivity we normally encounter in material science. By the way, this effective conductivity may well be characterized as an effective permeability coefficient[5] $P_e$ for the charge permeation by carriers through an oppositely charged background, i.e.,

$$P_e=R_{\rm CP}L_x/A , \tag{7}$$

where $A$ is the permeating area ($A=L_y$). If the permeation rate $R_{\rm CP}$ is equivalent to the charge current, then Eqs. (6) and (7) are equivalent to each other.

### C. Dependence of conductivity on concentration

Estimates for the effective conductivity are made over almost the whole range of concentration at several temperatures. The result for the variation of the conductivity with concentration $p$ is presented in Fig. 5. First of all, we note that, at a fixed temperature, the conductivity depends nomonotonically on the carrier concentration. At a low temperature, say, $\tau=0.01$, on increasing the concentration, the conductivity increases, reaching a maximum around $p_1^*=0.25$, followed by a decline in its magnitude with a kink in the curve around $p_2^*=0.60$. Let us call the first peak at $p_1^*$ the primary and that at $p_2^*$, the

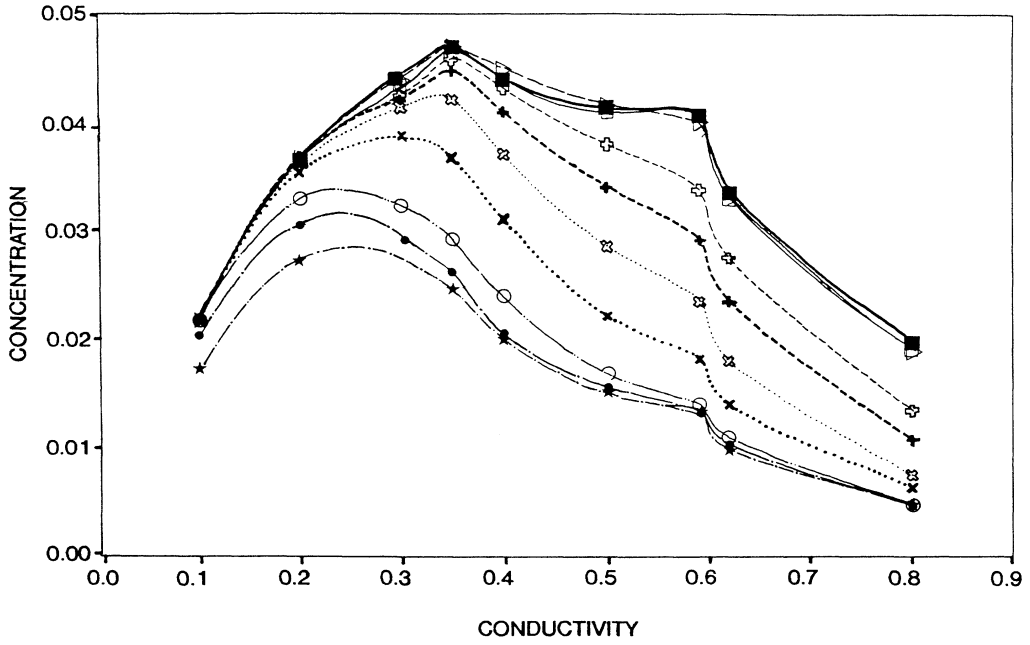


FIG. 5. Effective conductivity vs concentration at temperatures $\tau=0.01$ (★), 0.10 (●), 0.20 (○), 0.40 (×), 0.60 (⊠), 080 (+), 1.00 (✠), 2.00 (▽), 5.00 (■), and 10.00 (□). Up to half million time steps were used on a sample size $60\times60$.

secondary peak which is near the static percolation threshold. On raising the temperature, the primary peak shifts towards higher concentrations while the secondary peak remains at the percolation threshold of carrier concentration (see Fig. 5). Furthermore, both peaks become comparable at high temperatures (i.e., $\tau\geq10.00$).

The movement of particles is comparatively less hindered by their neighboring particles at low carrier concentration than at high concentrations. The probability of finding an empty site, for a particle to hop, is higher at lower carrier concentrations. It seems appropriate to assume that, at low concentrations, the transport quantity like conductivity will be dominated by the concentration of the empty sites, i.e., by the background charges. Therefore, the primary peak $p_1^*$ in conductivity should be close to the percolation threshold of empty sites (i.e., $1-p_2^*=0.592$). From Fig. 5 we observe that it varies between 0.25 and 0.40, depending on temperature. Furthermore, the primary peak is not as sharp as the secondary peak; it is rather broad, especially at low temperatures. One may interpret this peak as due to a percolation mechanism of the background charges which is smeared by the temperature and interactions. Nevertheless, this system exhibits the conductivity of a binary percolating system in which the background charges are dominant at low carrier concentration (leading to a primary peak at $p_1^*$) while the conductivity is limited by the carriers at high concentrations with a peak at $p_2^*$. The whole percolating mechanism may be referred to as an interacting dynamic percolation.

### D. Dependence of conductivity on temperature

The variation of conductivity with temperature is presented in Fig. 6. At a fixed carrier concentration, we observe that the conductivity remains constant, say, $\sigma_1$, in the low-temperature regime, and it saturates to a higher value, say, $\sigma_2$, in the high-temperature regime. In the intermediate regime, however, the conductivity increases with temperature from its minimum ($\sigma_1$) to a maximum value ($\sigma_2$). One usually looks[4] for an Arrhenius dependence whenever a temperature dependence of the transport quantities is involved, i.e., in our intermediate-temperature range,

$$\sigma = A\exp(-E_a/\tau)\ , \tag{8}$$

where $A$ is a constant and $E_a$ is an activation energy. A $\log\sigma$ versus $1/\tau$ plot for the intermediate regime is presented in Fig. 7. Our data at high concentration ($p=0.62$) show a linear fit (in the range $\tau^{-1}\sim0.1-2.0$) followed by an exponential-like decay to a different linear regime at extreme values of $\tau^{-1}$ (see Fig. 7). Slopes of the two linear fits lead to different activation energies in these temperature regimes; such a crossover in activation energy has been recently observed in the diffusion of plasticizers in PVC.[4] On increasing the concentration, it appears that the first Arrhenius regime reduces and the second regime expands. From the variation of our data (at low concentrations), even the validity of the Arrhenius dependence may be questioned. However, within the range of the validity of the Arrhenius dependence, as we see (Fig.

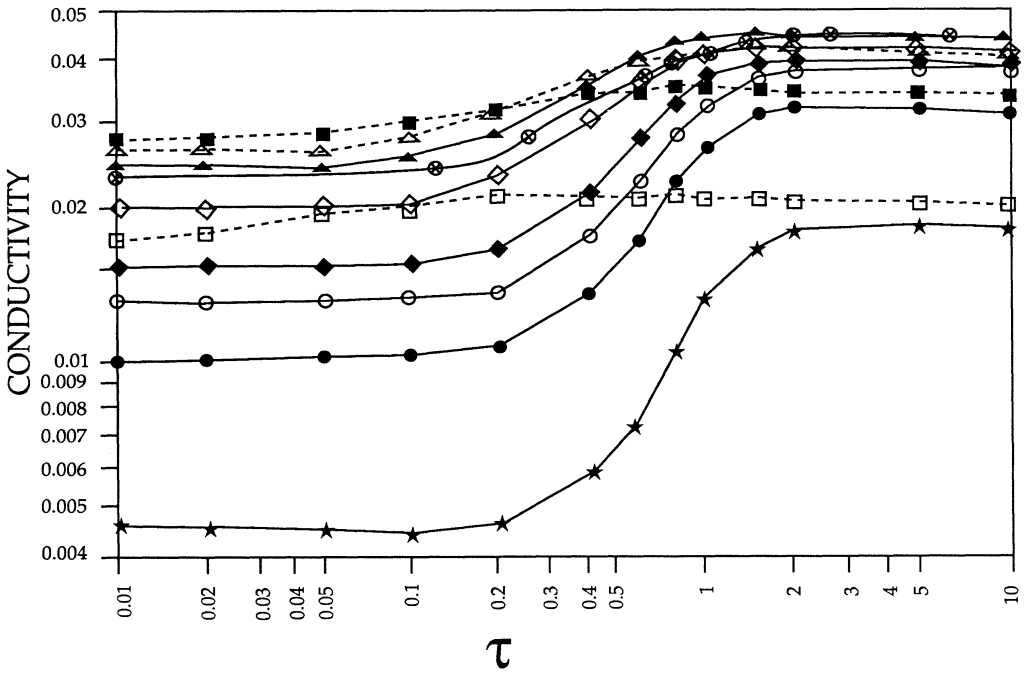


FIG. 6. Effective conductivity vs temperature on a log-log plot at concentration $p=0.10$ (□), 0.20 (■), 0.30 (▷), 0.35 (▶), 0.40 (◇), 0.50 (◆), 0.59, (○), 0.62 (●), and 0.80 (★) on a 60×60 sample. A set of data at $p=0.35$ (⊗) with sample size 40×40 is included to show that the finite size of the sample does not affect the qualitative nature of the steady-state transport properties.

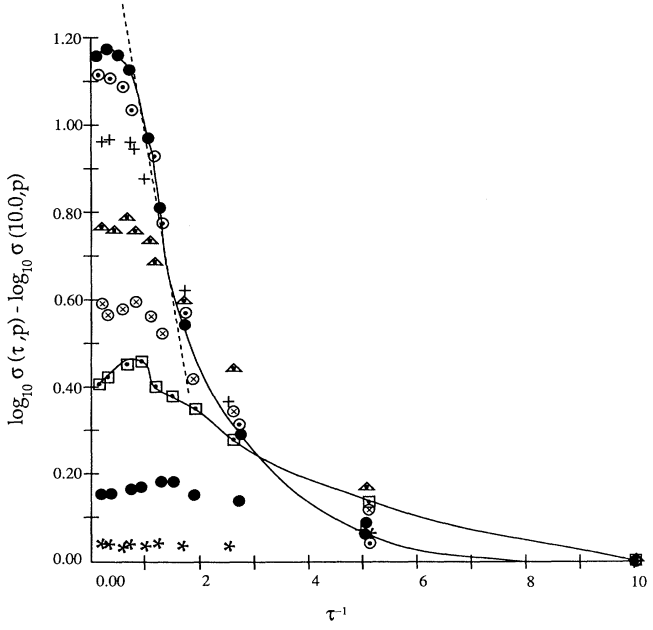


FIG. 7. Log ($\sigma$) vs inverse temperature ($1/\tau$) at concentration $p=0.10$ (★), 0.20 (●), 0.30 (□), 0.35 (⊗), 0.40 (△), 0.50 (+), 0.59 (○), and 0.62 (●, with line).

7), the activation energy depends on the carrier concentration. Our data suggest that the activation energy $E_a$ decreases on reducing the concentration. Further, we note that the difference in saturation values of the conductivity, i.e., $\sigma_2-\sigma_1$, shows a nonmonotonic behavior as a function of carrier concentration with a maximum around the percolation threshold ($p_c \sim 0.59$).

## IV. SUMMARY AND CONCLUSIONS

We have used MC simulation to study the transport properties of an interacting-lattice-gas model in two dimensions, in which a nearest-neighbor interaction among the particles and the host substrate is considered. The particles execute their stochastic motion with a hopping mechanism governed by the Metropolis algorithm. During the stochastic motion, as the particles reach one end (i.e., the source) of the lattice along the $x$ direction, they are charged with a unit charge density and they are discharged to zero charge density as soon as they reach the other end (i.e., the sink). A linear charge-density gradient is established in the steady-state equilibrium, and the whole system is maintained neutral by redistributing the background charge density to the substrate. Thus the charge is continuously transferred from source to sink by the charged particles, the carriers; the total charge (in

and out of the system) is conserved; and the validity of the continuity equation is maintained. This model may, therefore, capture some of the essential features of ionic transport in polymeric solution in an ionic solvent under a potential caused by either a charge-density gradient, mass density gradient, electrodes, or a combination of these parameters.

rms displacements of the tracers (i.e., the carriers) and that of their center of mass (for the collective motion) are studied. For the collective motion, the noise in the variation of the rms displacement $R_{\text{c.m.}}$ with time gives an idea about the ramification of the effective medium produced by the random distribution of the carriers and the charges and their interactions. The pattern of a systematic increase in its value followed by an abrupt decline gives an estimate of the time in which all the carriers are effective in transporting the charges across the sample; this may be useful in understanding the response properties, such as development of polarization and its decay in ionic solutions. The variation of the rms displacement $R_{\text{tr}}$ of the carriers with time exhibits two power-law behaviors: a slow mode in the short-time regime followed by a fast mode of driftlike motion in the long-time regime with a relaxation regime in between. The exponent $k_1$ characterizing the slow-mode motion is diffusive at low carrier concentration (i.e., in very dilute regime) and it seems to decrease with increasing the concentration $p$. The relaxation regime seems to expand on increasing the carrier concentration and lowering the temperature.

The effective conductivity $\sigma(p,\tau)$ depends nonmonotonically on the carrier concentration $p$ in which two peaks are observed. The primary peak at the lower concentration $p_1^*$ and the secondary peak at a higher concentration $p_2^*$ lend support for a two-percolation mechanism. It appears that the main mechanism that leads to the secondary peak is the site percolation. The secondary peak remains stable around the static-site percolation threshold $p_2^*$ except from the change in its magnitude as the temperature is varied. The primary peak, on the other hand, seems to arise from an interaction mechanism emerging from the carrier concentration, background charge density of the substrate, and temperature. The position of the primary peak $p_1^*$ shows a shift towards a higher value (but still lower than $p_2^*$) on raising the temperature. The two peaks become comparable at higher temperature ($\tau > 1.5$). We should point out that a mixture of two components (say, with different conductivity) gives rise to two percolation thresholds, a polychromatic percolation phenomenon.

There are three regimes of temperature in which the conductivity varies in its magnitude. At the low- and high-temperature regimes, it saturates to $\sigma_1$ and $\sigma_2$, respectively. The difference in these two extreme values, i.e., $\Delta\sigma(=\sigma_2-\sigma_1)$, decays down continuously on decreasing the carrier concentration $p$. In the intermediate-temperature regime, the conductivity seems to exhibit an Arrhenius dependence on temperature. The activation energy $E_a$ varies with the concentration and a crossover appears from high- to low-activation energies on lowering the temperature.

## ACKNOWLEDGMENTS

We thank Ken Mauritz for valuable discussions. We acknowledge support from the computer center at the University of Southern Mississippi, where all the data were produced on a DPS-90 Honeywell machine. Financial support from the donors of the Petroleum Research Fund (Grant No. ACS-PRF 21587) administered by the American Chemical Society is also acknowledged.

*Present address: Department of Electronics and Instrumentation, University of Arkansas at Little Rock, Little Rock, AR 72204.

[1]H. Yoon, H. Kim, and H. Yu, Macromolecules **22**, 848 (1989); M. Hara, J. Yu, and A. H. Lee, *ibid.* **22**, 754 (1989); C. Qian, M. R. Asdjodi, H. G. Spencer, and G. B. Savitsky, *ibid.* **22**, 998 (1989).

[2]C. W. Lantman, W. J. Macknight, D. G. Peiffer, S. K. Sinha, and R. D. Lundberg, Macromolecules **20**, 1096 (1987).

[3]K. A. Mauritz, J. Macromol. Sci. Rev. Macromol. Chem. Phys. C **28**, 65 (1988); K. A. Mauritz and R. M. Fu, Macromolecules **21**, 1324 (1988).

[4]R. F. Storey, K. A. Mauritz, and B. D. Cox, Macromolecules **22**, 289 (1989).

[5]T. Sakai, H. Takenaka, N. Wakabayashi, Y. Kawami, and E. Torikai, J. Electrochem. Soc. **132**, 1328 (1985).

[6]H. Bottger and V. V. Bryksins, Phys. Status Solidi B **113**, 9 (1982).

[7]*Selected Papers on Noise and Stochastic Processes,* edited by N. Wax (Dover, New York, 1954).

[8]*Fluctuation Phenomena,* edited by E. W. Montroll and J. L. Lebowitz (North-Holland, Amsterdam, 1979).

[9]J. W. Haus and K. W. Kehr, Phys. Rep. **150**, 263 (1987).

[10]K. W. Kehr, K. Binder, and S. M. Reulein, Phys. Rev. B **39**, 4891 (1989).

[11]O. Paetzold, J. Stat. Phys. **61**, 495 (1990).

[12]S. Havlin and D. Ben-Avraham, Adv. Phys. **36**, 695 (1987).

[13]D. Stauffer, in *Introduction to Percolation Theory* (Francis and Taylor, London, 1985).

[14]G. S. Grest, I. Webman, S. A. Safran, and A. L. R. Bug, Phys. Rev. A **33**, 2842 (1986); A. L. R. Bug and Y. Gefen, *ibid.* **35**, 1301 (1987).

[15]A. R. Kerstein and R. B. Pandey, Phys. Rev. A **35**, 3575 (1987).

[16]M. Sahimi and V. L. Jue, Phys. Rev. Lett. **62**, 629 (1989).

[17]M. Rosso, J. F. Gouyet, and B. Sapoval, Phys. Rev. Lett. **57**, 3195 (1986).

[18]Y. Gefen and J. W. Halley, in *Kinetics of Aggregation and Gelation,* edited by F. Family and D. P. Landau (North-Holland, Amsterdam, 1984).

[19]R. B. Pandey, Phys. Rev. A **42**, 3363 (1990).

[20]J. W. Davis, P. A. Lee, and T. M. Rice, Phys. Rev. B **29**, 4260 (1984).

[21]*Monte Carlo Methods in Statistical Physics,* edited by K. Binder (Springer-Verlag, Berlin, 1986).